

Cortical and Hippocampal Atrophy in Patients with Autosomal Dominant Familial Alzheimer's Disease

Liana G. Apostolova^{a, b} Kristy S. Hwang^{a, b} Luis D. Medina^a Amity E. Green^e
Meredith N. Braskie^{a, b} Rebecca A. Dutton^c Jeffrey Lai^d Daniel H. Geschwind^a
Jeffrey L. Cummings^a Paul M. Thompson^{a, b} John M. Ringman^a

^aMary S. Easton Center for Alzheimer's Disease Research, Department of Neurology, and ^bLaboratory of Neuroimaging, UCLA School of Medicine, Los Angeles, Calif., ^cUCSF School of Medicine, University of California, San Francisco, Calif., and ^dAlbert Einstein College of Medicine, Bronx, N.Y., USA; ^eMonash University, Melbourne, Vic., Australia

Key Words

Familial Alzheimer's disease · Familial autosomal dominant Alzheimer's disease · Presenilin · Amyloid precursor protein · Hippocampal atrophy · Cortical atrophy · Mutation carriers

Abstract

Background: Both familial and sporadic Alzheimer's disease (AD) result in progressive cortical and subcortical atrophy. Familial autosomal dominant AD (FAD) allows us to study AD brain changes presymptomatically. **Methods:** 33 subjects at risk for FAD (25 for PSEN1 and 8 for APP mutations; 22 mutation carriers and 11 controls) and 3 demented PSEN1 mutation carriers underwent T₁-weighted MPRAGE 1.5T MRI. Using the hippocampal radial distance and cortical pattern matching techniques, we investigated the effects of carrier status and dementia diagnosis on cortical and hippocampal atrophy. All analyses were corrected for age and relative age (years to median age of disease onset in the family). **Results:** The dementia cases had pronounced cortical atrophy in the lateral and medial parietal, posterior cingulate and frontal cortices and hippocampal atrophy bilaterally relative to both nondemented carriers and controls. Nondemented carriers

did not show significant cortical thinning or hippocampal atrophy relative to controls. **Conclusions:** FAD is associated with thinning of the posterior association and frontal cortices and hippocampal atrophy. Larger sample sizes may be necessary to reliably identify cortical atrophy in presymptomatic carriers.

Copyright © 2011 S. Karger AG, Basel

Introduction

Familial autosomal dominant Alzheimer's disease (FAD) accounts for less than 2% of all Alzheimer's disease (AD) cases but offers unique insight into the presymptomatic stages of the disorder. FAD results from fully penetrant autosomal dominant mutations of 1 of 3 genes – presenilin 1 (PSEN1), presenilin 2 (PSEN2) and the amyloid precursor protein (APP) or duplication of the APP gene [1–3]. Hence, once genotyped, we can predict with a very high level of certainty which family members will develop AD. Several lines of evidence [4–9] suggest that FAD subjects may exhibit brain atrophy several years prior to transition to overt dementia. Greater baseline hippocampal atrophy and greater rates of hippocampal

and regional cortical atrophy have been reported in a group of 2 APP and 3 PSEN1 [9] and in a group of 3 APP mutation carriers [5] at the time of clinical presentation. Progressive hippocampal atrophy starting as early as 9 years prior to dementia diagnosis was reported in a single APP mutation case [10]. A small study of 5 APP and 4 PSEN1 carriers [8] described hippocampal atrophy as an earlier and global cortical atrophy as a later phenomenon. A cross-sectional comparison of mutation carriers and cognitively normal controls revealed differences in hippocampal volume in the mild cognitive impairment (MCI) stage, while whole brain volume differed only once subjects transitioned to overt dementia. Yet once the longitudinal rate of change was closely inspected, higher atrophy rates were noted as early as 5.5 years prior to clinical diagnosis for the hippocampus and 3.5 years for whole brain volume in mutation carriers relative to controls [8]. Applying the region-of-interest approach, the same group later reported that cortical atrophy in selected regions – the precuneus and posterior cingulate – was present 4.1 and 1.8 years prior to dementia diagnosis, respectively [7]. Finally, left-sided posterior cortical atrophy was reported in another small group of 6 nondemented PSEN1 carriers of whom 5 already exhibited memory decline [6].

As FAD has a very low prevalence, all structural imaging studies to date have included between 1 [10] and 10 FAD mutation carriers [11]. Here we report structural MRI analyses of 25 mutation carriers – 3 demented and 22 who were either cognitively normal ($n = 15$) or with mild memory problems ($n = 7$), and compared them to 11 subjects from the same families who tested negative for their respective familial pathogenic mutation. In the current study, we sought to define cortical and hippocampal atrophy in an independent cohort of persons at risk for FAD using different analytical techniques. We hypothesized that we would be able to detect hippocampal and cortical atrophy in older, yet still presymptomatic FAD mutation carriers.

Methods

Subjects

Our subject pool consisted of 37 subjects from families known to harbor pathogenic FAD mutations. There were 33 nondemented and 3 demented subjects from 10 families with PSEN1 mutations and 2 families with V717I APP mutation. The 10 PSEN1 families included 1 with L235V [12], 1 with G206A [13], and 7 with A431E substitution (founder effect originating in Jalisco State in Mexico [14, 15]). Subjects who tested positive for the mutation will be referred to as carriers and subjects who tested negative for the mutation will be referred to as controls.

The subject's cognitive status was characterized using the neuropsychological battery available in both English and Spanish detailed in Ringman et al. [16]. Composite z-scores were calculated for each of the four domains of each mutation carrier using the mean domain scores of nonmutation carriers. The four domains consisted of language (category fluency for animals, Object Naming from the Spanish-English Neuropsychological Assessment Scale [17]), visuospatial (Rey-Osterrieth Figure Copy [18], Block Design from the WMS-R [19]), verbal memory (Word List Learning Delayed Recall, Memory Verbal Prose Delayed Recall [20]) and frontal/executive function (Stroop Interference Score [21], Color Trails Interference Score). Mutation carriers who scored 1.5 standard deviations or more below noncarriers on these composite scores were defined as being impaired in that domain.

Clinical status was defined using the Clinical Dementia Rating Scale (CDR) and Petersen's criteria for MCI [22]. A CDR score of 0 indicates asymptomatic, 0.5 questionable demented, 1 mildly demented, 2 moderately demented, and 3 severely demented clinical state [23]. CDR evaluations were performed blinded to subject's mutation status except in the cases of overtly demented subjects. All 3 demented (CDR score ≥ 1) and 7 of 9 (78%) mildly symptomatic subjects (CDR score = 0.5) were mutation carriers. Of the 24 asymptomatic subjects (CDR score = 0), 15 (62.5%) carried pathogenic APP or PSEN1 mutations. One mutation carrier with a CDR score of 0 met Petersen's criteria for MCI.

Subjects' ages ranged from 19 to 54 years. As the age of onset is relatively consistent within any given family [15], relative age was defined as the difference between the median age of dementia diagnosis for the family and each subject's age. Relative age ranged from -35 to +2 years (i.e., from 35 years prior to 2 years after the median age of dementia diagnosis for the respective family).

Genetic Testing

DNA was extracted and apolipoprotein E genotyping performed using standard techniques. The presence of the A431E, L235V, and G206A substitutions in PSEN1 were assessed using restriction fragment length polymorphism analyses. The presence of the V717I substitution in APP was assessed with direct sequencing.

Imaging Data Acquisition and Analyses

T_1 -weighted brain images were obtained on the same 1.5T Siemens Sonata scanner in the sagittal plane using a 3D MPRAGE sequence (TR = 1,900 ms, TE = 4.38 ms, TI = 1,100 ms, flip angle 15°, voxel size of $1 \times 1 \times 1$ mm³). All images were linearly registered to the International Consortium for Brain Mapping space [24]. Intensity nonuniformity correction was applied [25]. One experienced rater (intrarater variability: Cronbach's alpha = 0.97) manually traced the hippocampal formations in the coronal plane following our extensively validated manual tracing protocol and in consultation with two detailed published hippocampal atlases [26, 27]. Three-dimensional hippocampal parametric mesh models were computed. The central core of each hippocampal structure, defined as the medial curve threading down the centroid of each hippocampus, was derived. The radial distance (i.e., the distance from the central core to each surface point) was determined and digitally recorded at each three-dimensional coordinate location of the hippocampal mesh models [28].

We used BrainSuite [25] to generate whole brain masks from the spatially and intensity-corrected three-dimensional 1.5T MR

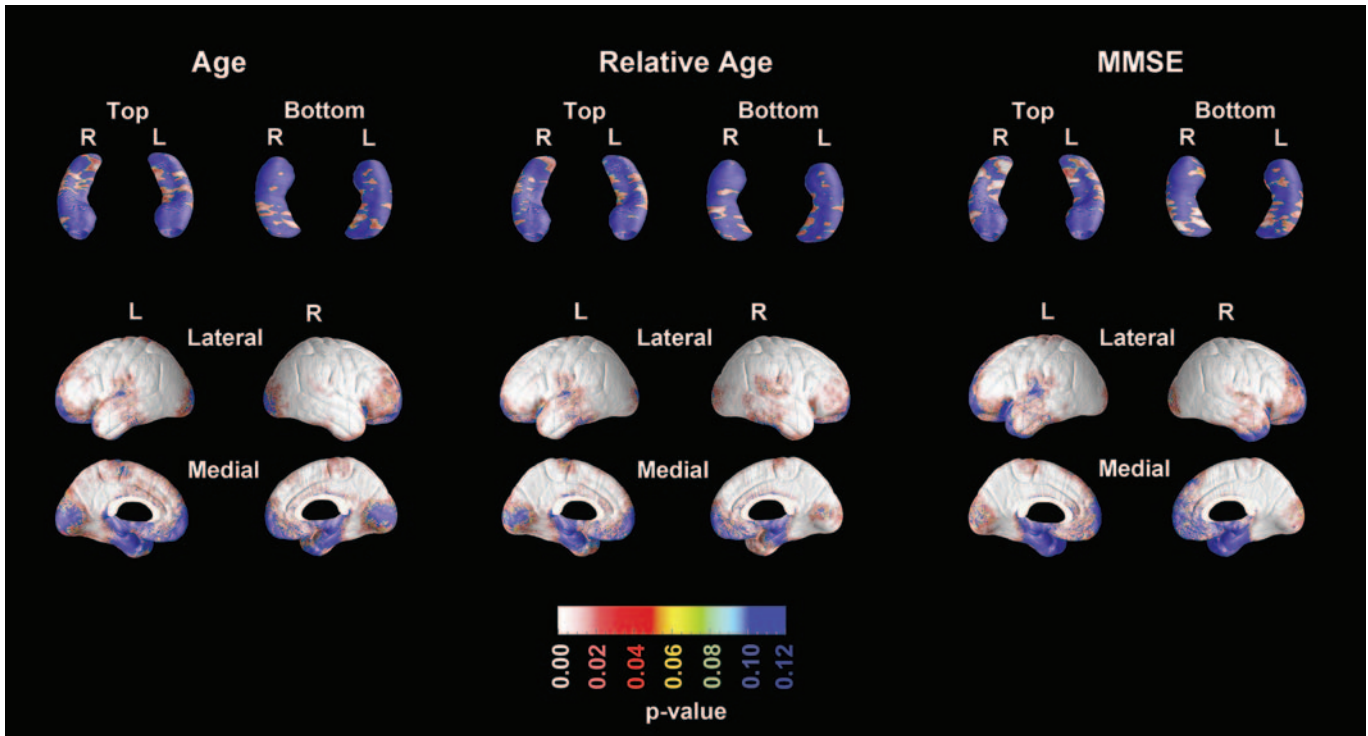


Fig. 1. Associations between age, relative age and MMSE scores and hippocampal radial distance or cortical thickness in the pooled sample.

images. These masks were visually inspected and all misidentified brain and nonbrain tissue correctly labeled. Separate left and right hemispheric masks and three-dimensional hemispheric reconstructions were produced. Thirty-eight sulci per hemisphere were traced following our detailed, extensively validated protocol [29]. Individual sulcal maps were averaged to create a common study-specific average sulcal template. Individual hemispheric surfaces were parameterized, flattened and warped so that the individual sulci align with the respective average sulcal representations (a technique known as cortical pattern matching). This step ensures as precise as possible a matching of homologous gyri prior to analyzing the cortical thickness data and conducting statistical comparisons [30].

Next, we used BrainSuite to segment the T_1 -weighted MR images into three tissue types – gray matter, white matter and cerebrospinal fluid. We then computed the three-dimensional distance from the gray matter/white matter to the gray matter/cerebrospinal fluid interface at each surface point for each individual. The gray matter thickness values, in millimeters, were plotted at each point on the parametric cortical surface model. To combine thickness data across subjects, data from corresponding cortical regions were averaged together using the cortical pattern matching technique [30, 31]. With each subject's thickness data aligned as precisely as possible, we were able to fit statistical models with cortical thickness as the dependent variable at each cortical surface point.

We verified our results for nondemented carriers versus non-carriers using voxel-based morphometry as implemented in a fre-

quently employed software package (FSL 4.1.7). Each subject was nonlinearly aligned to a study-specific template composed of all noncarriers and an equal number of nondemented carriers who were randomly selected. Data were analyzed using a threshold-free cluster enhancement-based method, which enhances clusters but results in a comparison that retains elements of voxel-wise comparisons. Threshold-free cluster enhancement allows comparisons to be made using relatively small smoothing kernels; we used a Gaussian kernel of 4 mm full width at half maximum. Multiple comparisons were controlled using 10,000 permutations, which provides a confidence interval of 0.0500 ± 0.0044 .

Statistical Methods

We used two-tailed independent-sample t tests and χ^2 tests to compare the demographic variables between the groups for each diagnostic comparison (nondemented carriers vs. demented carriers; demented carriers vs. controls and nondemented carriers vs. controls). We used linear regression models to study the effect of diagnosis – or in the case of nondemented subjects, carrier status – on cortical thickness and hippocampal radial distance, while adjusting for age and relative age. Both age and relative age showed highly significant effects on hippocampal and cortical thickness (fig. 1, left and middle panel). Next we divided the nondemented carrier group into three subgroups – those with relative age <10 years ($n = 8$), 10–20 years ($n = 10$) and >20 years ($n = 4$). We compared each group to our controls ($n = 11$) in a similar fashion as described above. In addition, we also compared all carriers

with a CDR score = 0 ($n = 15$) and all carriers with a CDR score = 0.5 ($n = 7$) to our noncarriers with a CDR score = 0 ($n = 9$). Using linear regression, we also investigated the association between Mini-Mental State Examination (MMSE) scores and hippocampal atrophy or cortical thinning in the pooled sample (fig. 1, right panel). The final results (fig. 2–3) are displayed as three-dimensional statistical maps with regions of significance ($p < 0.05$) color-coded in red to white.

The overall significance of the statistical maps was assessed using permutation methods. These randomly permute the main predictor variable (i.e., diagnosis or carrier status) and then test whether the fraction of the cortical or hippocampal surface area with statistics exceeding a given fixed threshold (in our case $p < 0.01$) seen in the true experiment exceeds what would be expected by chance from the random data. As we have done previously, we conducted 100,000 random permutations for each analysis [30].

Results

There were no differences in age, MMSE or global CDR scores between nondemented carriers and controls (table 1). On average, nondemented carriers were 13.7 years younger and noncarriers were 12.3 years younger than the median age of disease diagnosis for their family (i.e., relative age -13.7 and -12.3 years, respectively). This difference was not statistically significant. Compared to controls and nondemented carriers, demented carriers were significantly older, had significantly lower MMSE and higher global CDR scores ($p < 0.05$ for all). The three groups were well balanced with respect to gender.

As shown in the left and middle panel of figure 1, we found trend-level effects of age and relative age on right hippocampal radial distance (age: left $p > 0.05$; right $p = 0.06$; relative age: left $p > 0.05$, right $p = 0.09$) and significant effects on cortical thickness bilaterally (age: left $p_{\text{corrected}} = 0.0067$, right $p_{\text{corrected}} = 0.0022$; relative age: left $p_{\text{corrected}} = 0.0039$, right $p_{\text{corrected}} = 0.002$). All subsequent statistical analyses were thus corrected for age and relative age.

Hippocampal Analyses

We found no significant differences in hippocampal radial distance between nondemented carriers and controls in our three-dimensional age- and relative age-adjusted hippocampal linear regression analyses (fig. 2, top row). The subgroup comparisons of mutation carriers grouped by relative age (<10 , $10-20$ and >20 years) to our control subjects did not reveal any statistically significant results. Similarly, comparing carriers with a CDR score = 0 to controls with a CDR score = 0 and carriers with a

CDR score = 0.5 to controls with a CDR score = 0 did not reveal any significant differences.

The three-dimensional age- and relative age-adjusted statistical maps showed significant hippocampal atrophy in demented carriers relative to controls on the right (left $p_{\text{corrected}} > 0.05$; right $p_{\text{corrected}} = 0.047$). The areas of significant differences demonstrated up to 60% greater atrophy in demented subjects (fig. 3, top row). As expected, MMSE showed highly significant positive associations with hippocampal radial distance bilaterally (left $p_{\text{corrected}} = 0.0034$; right $p_{\text{corrected}} = 0.00031$; fig. 1, top right panel).

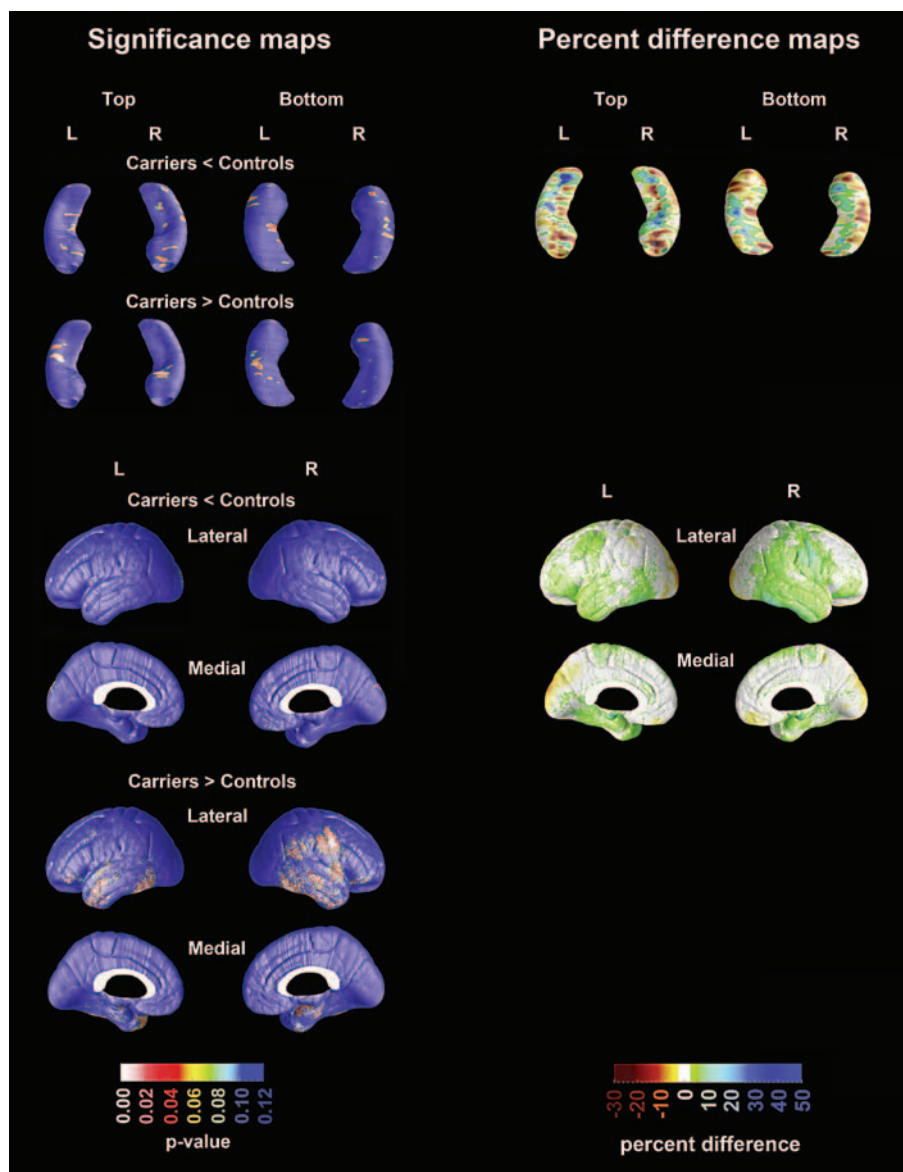
Cortical Analyses

We detected no significant cortical thinning in nondemented carriers relative to controls. While there were few areas where nondemented carriers showed thicker cortex relative to controls, these results did not survive stringent correction for multiple comparisons (fig. 2). These results remained unchanged after we reanalyzed the data using FSL. The subgroup comparisons of mutation carriers grouped by relative age (<10 years, $10-20$ years and >20 years) to our control subjects did not reveal any statistically significant results. Similarly, comparing carriers with a CDR score = 0 to controls with a CDR score = 0 and carriers with a CDR score = 0.5 to controls with a CDR score = 0 did not reveal any significant differences.

The demented carriers showed significant thinning of the parietal, parieto-occipital, precuneus and posterior cingulate cortices relative to controls (left $p_{\text{corrected}} = 0.028$; right $p_{\text{corrected}} = 0.033$; fig. 3, top panel). The differences in cortical thickness were more pronounced in demented versus nondemented mutation carriers likely driven by the fact that our nondemented carriers showed a tendency for thicker cortex when compared to our controls (left $p_{\text{corrected}} = 0.016$; right $p_{\text{corrected}} = 0.0048$; fig. 3, bottom panel). As expected, MMSE scores showed extensive and highly significant positive associations with cortical thickness throughout the cortex except for the entorhinal/perihippocampal area (left $p = 0.0039$; right $p = 0.002$; fig. 1, top right panel).

Discussion

It is now well accepted that in late-onset sporadic AD the pathologic hallmarks of the disorder begin accumulating years and perhaps even decades before the first clinical symptoms appear [32, 33]. In vivo structural im-



Color version available online

Fig. 2. Hippocampal and cortical thickness three-dimensional statistical maps comparing nondemented mutation carriers with controls (relative age -12.3 vs. -13.7 years, respectively).

Table 1. Demographic data

	Nondemented controls (n = 11)	Nondemented carriers (n = 22)	Demented carriers (n = 3)
Age, years	35.2 (7.8)	32.2 (7.5)	48.3 (5.5)
Relative age, years	-12.3 (10.6)	-13.7 (8.7)	2.7 (3.1)
Gender (M/F)	2/9	4/18	1/2
ApoE4+/-	2/9	2/20	0/3
MMSE score	28.1 (1.8)	27.6 (2.4)	8.3 (4.9)
Global CDR score	0.09 (0.2)	0.16 (0.2)	2.3 (0.6)
PSEN1 A431E, n	5	14	1
PSEN1 L235V and 206A, n	3	3	2
APP V717I, n	3	5	0

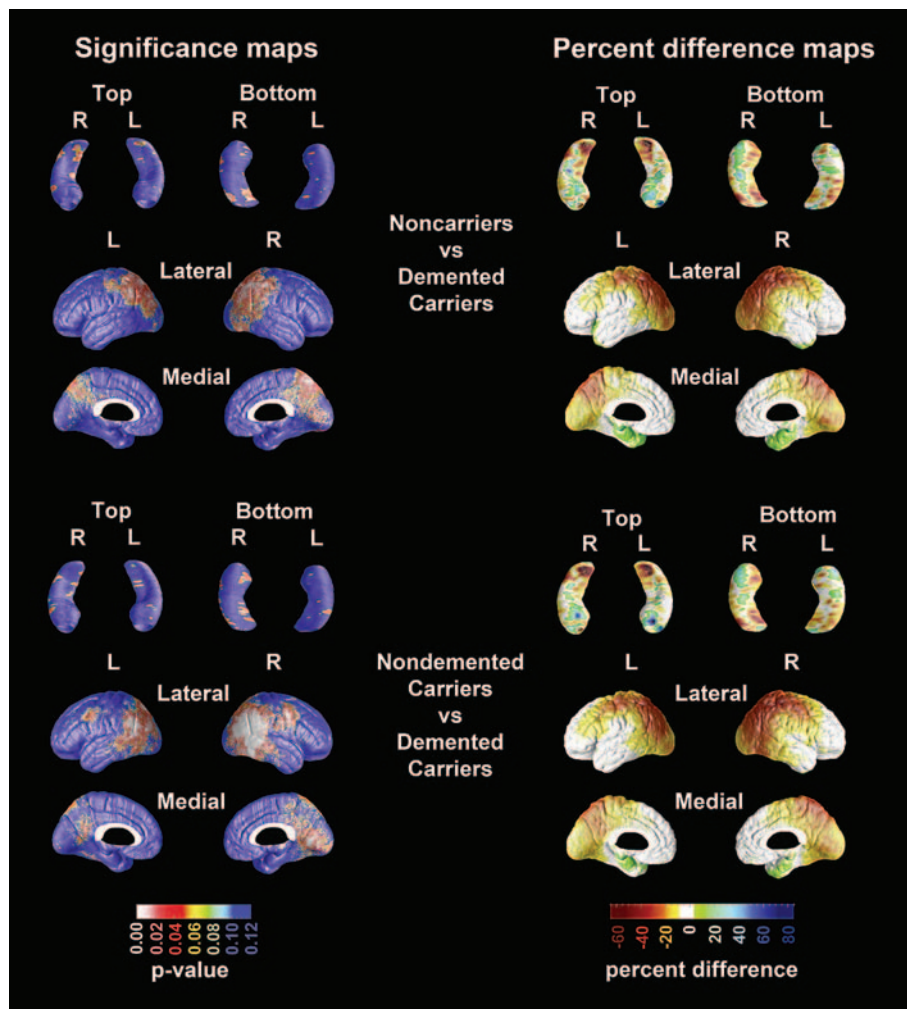


Fig. 3. Hippocampal and cortical thickness three-dimensional statistical maps comparing demented carriers with controls and nondemented carriers.

aging shows of sporadic AD subjects show progressive hippocampal [28, 34, 35] and cortical loss [30, 36], and global brain atrophy [37, 38].

Presymptomatic and early symptomatic but not yet demented FAD mutation carriers offer an opportunity to investigate the clinical and biomarker substrate of the prodromal dementia stages. As FAD has a very low prevalence, all structural imaging studies to date have included between one [10] and 10 FAD mutation carriers [11]. Here we report structural MRI analyses of 25 mutation carriers – 3 demented and 22 who were either cognitively normal (n = 15) or with mild memory problems (n = 7), and compared them to 11 subjects from the same families who tested negative for their respective familial pathogenic mutation.

Our FAD demented subjects showed pronounced and widespread cortical atrophy with cortical thinning ap-

proaching 60% as well as significant hippocampal atrophy in some areas in the parietal and precuneal regions relative to both FAD noncarriers and FAD nondemented carriers. Hence our study supports and extends previously reported findings. Similar to others, we found gray matter atrophy in the posterior cingulate [11] and the temporal and parietal association cortices [6] in demented FAD subjects (fig. 3). The pattern of hippocampal atrophy seen in demented FAD subjects (fig. 3) resembles that observed in sporadic AD [35, 39]. Our inability to detect significant hippocampal atrophy during the presymptomatic phase of the disease in FAD mutation carriers in the current study is consistent with radiologists' inability to visually detect such changes in the same population in a prior report [40].

Contrary to our main hypothesis, we failed to find cortical or hippocampal atrophy in our nondemented muta-

tion carriers. This prompted a very careful investigation of the intermediate imaging files generated during both pre- and postprocessing and led to the determination that the lack of significant atrophy in nondemented mutation carriers was not due to segmentation failure, movement artifacts or any other technical issues. This may suggest that FAD is a complicated heterogeneous disorder with some mutations leading to pronounced early cortical and hippocampal changes, while others do not. We did repeat our analyses using the VBM approach, which has been used by others reporting brain atrophy in FAD, but that approach confirmed our negative findings.

The suggestion for thicker cortex in nondemented mutation carriers relative to controls is interesting. As noted above, these findings were not due to technical issues. As these findings did not survive correction for multiple comparisons, they should be interpreted with caution. Should this observation be validated in an independent sample, one might want to consider the possibility of cortical maldevelopment caused by the presence of autosomal dominant AD mutations, which results in aberrant thicker cortical morphology.

A prior study by our group used diffusion tensor imaging to measure fractional anisotropy in FAD mutation carriers, and included a subset of the subjects ($n = 23$) from the current study. That study found lower fractional anisotropy in the columns of the fornix, perforant pathways, left orbitofrontal gyri and mean whole brain white matter among mutation carriers [41]. This may suggest that, in FAD, changes in white matter integrity occur prior to detectable volumetric changes in the cortex. While the exact pathological changes underlying white matter deterioration in FAD remain to be fully elucidated, a process other than axonal degeneration from cortical and hippocampal neuron loss might underlie the findings reported previously.

Several strengths and limitations of our study should be recognized. This is one of the largest structural imaging analyses of FAD mutation carriers to date. Even so,

we did not observe significant cortical or hippocampal atrophy in nondemented FAD mutation carriers relative to controls. There are several plausible explanations for this. One is that an even larger and better balanced sample may be needed to detect statistically significant between-group differences. An alternative explanation could be the variability introduced by the very broad relative age range in our study (-35 to $+2$ years). A more homogeneous study sample in terms of relative age may improve our power to detect early disease-associated changes. Alternatively, larger sample sizes might allow us to separate the groups based on relative age and study the disease effects in subgroups with similar time to average age of disease onset. Finally a longitudinal protocol may offer the best strategy to study disease changes over time and demonstrate the earliest changes in the presymptomatic stage. Our CDR raters who were blinded to genetic status gave 2 nonmutation carriers a CDR score of 0.5. Additionally, 1 mutation carrier with a CDR score of 0 met Petersen's criteria for MCI. This could indicate that either the CDR measurement lacks precision or that some subjects from these families could have cognitive complaints and problems not related to mutation status. We are presently following these subjects and collecting longitudinal clinical, cognitive and imaging data at UCLA as well as as part of the Dominantly Inherited Alzheimer Network (<http://www.dian-info.org/>).

Acknowledgments

This study was supported by the Easton Consortium for Alzheimer Disease Drug Discovery and Biomarker Development, NIA K23 AG026803, NIA P50 AG16570, NIBIB EB008561, NIBIB EB01651, NLM LM05639, NCRR RR019771; NIH RR021813, PHS K08 AG-22228, M01-RR00865, California DHS No. 04-35522, the Goldberg Trust, and the Sidell-Kagan Foundation. P.M.T. was also supported by EB008281, EB008432, AG020098, and P41 RR013642.

References

- 1 Rovelet-Lecrux A, Hannequin D, Raux G, Le Meur N, Laquerriere A, Vital A, Dumanchin C, Feuillet S, Brice A, Vercelletto M, Dubas F, Frebourg T, Campion D: APP locus duplication causes autosomal dominant early-onset Alzheimer disease with cerebral amyloid angiopathy. *Nat Genet* 2006;38:24–26.
- 2 Chartier-Harlin MC, Crawford F, Houlden H, Warren A, Hughes D, Fidani L, Goate A, Rossor M, Roques P, Hardy J, et al: Early-onset Alzheimer's disease caused by mutations at codon 717 of the beta-amyloid precursor protein gene. *Nature* 1991;353:844–846.
- 3 Sherrington R, Rogaeve EI, Liang Y, Rogaeve EA, Levesque G, Ikeda M, Chi H, Lin C, Li G, Holman K, Tsuda T, Mar L, Foncin JF, Bruni AC, Montesi MP, Sorbi S, Rainero I, Pinessi L, Nee L, Chumakov I, Pollen D, Brookes A, Sanseau P, Polinsky RJ, Wasco W, Da Silva HA, Haines JL, Pericak-Vance MA, Tanzi RE, Roses AD, Fraser PE, Rommens JM, St George-Hyslop PH: Cloning of a gene bearing missense mutations in early-onset familial Alzheimer's disease. *Nature* 1995;375:754–760.
- 4 Fox NC, Crum WR, Scahill RI, Stevens JM, Janssen JC, Rossor MN: Imaging of onset and progression of Alzheimer's disease with voxel-compression mapping of serial magnetic resonance images. *Lancet* 2001;358:201–205.

- 5 Fox NC, Warrington EK, Freeborough PA, Hartikainen P, Kennedy AM, Stevens JM, Rossor MN: Presymptomatic hippocampal atrophy in Alzheimer's disease. A longitudinal MRI study. *Brain* 1996;119:2001–2007.
- 6 Ginestroni A, Battaglini M, Della Nave R, Moretti M, Tessa C, Giannelli M, Caffarra P, Nacmias B, Bessi V, Sorbi S, Bracco L, De Stefano N, Mascalchi M: Early structural changes in individuals at risk of familial Alzheimer's disease: a volumetry and magnetization transfer MR imaging study. *J Neurol* 2009;256:925–932.
- 7 Knight WD, Kim LG, Douiri A, Frost C, Rossor MN, Fox NC: Acceleration of cortical thinning in familial Alzheimer's disease. *Neurobiol Aging*, E-pub ahead of print.
- 8 Ridha BH, Barnes J, Bartlett JW, Godbolt A, Pepple T, Rossor MN, Fox NC: Tracking atrophy progression in familial Alzheimer's disease: a serial MRI study. *Lancet Neurol* 2006;5:828–834.
- 9 Schott JM, Fox NC, Frost C, Scahill RI, Janssen JC, Chan D, Jenkins R, Rossor MN: Assessing the onset of structural change in familial Alzheimer's disease. *Ann Neurol* 2003;53:181–188.
- 10 Godbolt AK, Cipolotti L, Anderson VM, Archer H, Janssen JC, Price S, Rossor MN, Fox NC: A decade of pre-diagnostic assessment in a case of familial Alzheimer's disease: tracking progression from asymptomatic to MCI and dementia. *Neurocase* 2005;11:56–64.
- 11 Jones BF, Barnes J, Uylings HB, Fox NC, Frost C, Witter MP, Scheltens P: Differential regional atrophy of the cingulate gyrus in Alzheimer disease: a volumetric MRI study. *Cereb Cortex* 2006;16:1701–1708.
- 12 Janssen JC, Beck JA, Campbell TA, Dickinson A, Fox NC, Harvey RJ, Houlden H, Rossor MN, Collinge J: Early onset familial Alzheimer's disease: mutation frequency in 31 families. *Neurology* 2003;60:235–239.
- 13 Athan ES, Williamson J, Ciappa A, Santana V, Romas SN, Lee JH, Rondon H, Lantigua RA, Medrano M, Torres M, Arawaka S, Rogava E, Song YQ, Sato C, Kawarai T, Fafel KC, Boss MA, Seltzer WK, Stern Y, St George-Hyslop P, Tycko B, Mayeux R: A founder mutation in presenilin 1 causing early-onset Alzheimer disease in unrelated Caribbean Hispanic families. *JAMA* 2001;286:2257–2263.
- 14 Yescas P, Huertas-Vazquez A, Villarreal-Molina MT, Rasmussen A, Tusie-Luna MT, Lopez M, Canizales-Quinteros S, Alonso ME: Founder effect for the ala431glu mutation of the presenilin 1 gene causing early-onset Alzheimer's disease in Mexican families. *Neurogenetics* 2006;7:195–200.
- 15 Murrell J, Ghetti B, Cochran E, Macias-Islas MA, Medina L, Varpetian A, Cummings JL, Mendez MF, Kawas C, Chui H, Ringman JM: The A431E mutation in PSEN1 causing familial Alzheimer's disease originating in Jalisco State, Mexico: an additional fifteen families. *Neurogenetics* 2006;7:277–279.
- 16 Ringman JM, Medina LD, Rodriguez-Agudelo Y, Chavez M, Lu P, Cummings JL: Current concepts of mild cognitive impairment and their applicability to persons at risk for familial Alzheimer's disease. *Curr Alzheimer Res* 2009;6:341–346.
- 17 Mungas D, Reed BR, Crane PK, Haan MN, Gonzalez H: Spanish and English Neuropsychological Assessment Scales (SENAS): further development and psychometric characteristics. *Psychol Assess* 2004;16:347–359.
- 18 Osterrieth PA: Le test de copie d'une figure complexe. *Arch Psychol* 1944;30:206–356.
- 19 Wechsler D: Wechsler Memory Scale – Revised. San Antonio, The Psychological Corporation, 1987.
- 20 Artiola-i-Fortuny L, Hermsillo D, Heaton RK, Pardee RE: Manual de normas y procedimientos para la batería neuropsicología en español. Tuscon, Neuropsychology Press, 1999.
- 21 Stroop JR: Studies in interference of serial verbal reactions. *J Exp Psychol* 1935;18:643–662.
- 22 Petersen RC, Doody R, Kurz A, Mohs RC, Morris JC, Rabins PV, Ritchie K, Rossor M, Thal L, Winblad B: Current concepts in mild cognitive impairment. *Arch Neurol* 2001;58:1985–1992.
- 23 Morris JC: Clinical dementia rating: a reliable and valid diagnostic and staging measure for dementia of the Alzheimer type. *Int Psychogeriatr* 1997;9(suppl 1):173–176; discussion 177–178.
- 24 Mazziotta J, Toga A, Evans A, Fox P, Lancaster J, Zilles K, Woods R, Paus T, Simpson G, Pike B, Holmes C, Collins L, Thompson P, MacDonald D, Iacoboni M, Schormann T, Amunts K, Palomero-Gallagher N, Geyer S, Parsons L, Narr K, Kabani N, Le Goualher G, Boomsma D, Cannon T, Kawashima R, Mazoyer B: A probabilistic atlas and reference system for the human brain: International Consortium for Brain Mapping (ICBM). *Philos Trans R Soc Lond B Biol Sci* 2001;356:1293–1322.
- 25 Shattuck DW, Leahy RM: Brainsuite: an automated cortical surface identification tool. *Med Image Anal* 2002;6:129–142.
- 26 Duvernoy H: The Human Hippocampus. An Atlas of Applied Anatomy. Munich, JF Bergmann Verlag, 1988.
- 27 Mai JK, Paxinos G, Assheuer JK: Atlas of the Human Brain. San Diego, Elsevier Academic Press, 2004.
- 28 Thompson PM, Hayashi KM, De Zubicaray GI, Janke AL, Rose SE, Semple J, Hong MS, Herman DH, Gravano D, Dordrell DM, Toga AW: Mapping hippocampal and ventricular change in Alzheimer disease. *Neuroimage* 2004;22:1754–1766.
- 29 Hayashi KM, Thompson PM, Mega MS, Zoumalan CI: Medial hemispheric surface gyral pattern delineation in 3D: surface curve protocol. 2002. http://users.ionu.ucla.edu/~khayashi/Public/medial_surface/.
- 30 Thompson PM, Hayashi KM, de Zubicaray G, Janke AL, Rose SE, Semple J, Herman D, Hong MS, Dittmer SS, Dordrell DM, Toga AW: Dynamics of gray matter loss in Alzheimer's disease. *J Neurosci* 2003;23:994–1005.
- 31 Thompson PM, Hayashi KM, Sowell ER, Gogtay N, Giedd JN, Rapoport JL, de Zubicaray GI, Janke AL, Rose SE, Semple J, Dordrell DM, Wang Y, van Erp TG, Cannon TD, Toga AW: Mapping cortical change in Alzheimer's disease, brain development, and schizophrenia. *Neuroimage* 2004;23(suppl 1):S2–S18.
- 32 Haroutunian V, Perl DP, Purohit DP, Marin D, Khan K, Lantz M, Davis KL, Mohs RC: Regional distribution of neuritic plaques in the nondemented elderly and subjects with very mild Alzheimer disease. *Arch Neurol* 1998;55:1185–1191.
- 33 Price JL, Morris JC: Tangles and plaques in nondemented aging and 'preclinical' Alzheimer's disease. *Ann Neurol* 1999;45:358–368.
- 34 Apostolova LG, Dutton RA, Dinov ID, Hayashi KM, Toga AW, Cummings JL, Thompson PM: Conversion of mild cognitive impairment to Alzheimer disease predicted by hippocampal atrophy maps. *Arch Neurol* 2006;63:693–699.
- 35 Apostolova LG, Green AE, Hwang KH, Cummings JL, Toga AW, Thompson PM: Mapping hippocampal atrophy in mild cognitive impairment and Alzheimer's disease. 61st AAN Meeting, Seattle, 2009.
- 36 Apostolova LG, Steiner CA, Akopyan GG, Dutton RA, Hayashi KM, Toga AW, Cummings JL, Thompson PM: Three-dimensional gray matter atrophy mapping in mild cognitive impairment and mild Alzheimer disease. *Arch Neurol* 2007;64:1489–1495.
- 37 Chetelat G, Landeau B, Eustache F, Mezenge F, Viader F, de la Sayette V, Desgranges B, Baron JC: Using voxel-based morphometry to map the structural changes associated with rapid conversion in MCI: a longitudinal MRI study. *Neuroimage* 2005;27:934–946.
- 38 Karas GB, Scheltens P, Rombouts SA, Visser PJ, van Schijndel RA, Fox NC, Barkhof F: Global and local gray matter loss in mild cognitive impairment and Alzheimer's disease. *Neuroimage* 2004;23:708–716.
- 39 Apostolova LG, Thompson PM, Green AE, Hwang KS, Zoumalan C, Jack CR, Harvey D, Petersen RC, Thal LJ, Aisen PS, Toga AW, Cummings JL, DeCarli C: 3D comparison of low, intermediate and advanced hippocampal atrophy in MCI. *Hum Brain Mapp* 2010;31:786–797.
- 40 Ringman JM, Pope W, Salamon N: Insensitivity of visual assessment of hippocampal atrophy in familial Alzheimer's disease. *J Neurol* 2010;257:839–842.
- 41 Ringman JM, O'Neill J, Geschwind D, Medina L, Apostolova LG, Rodriguez Y, Schaffer B, Varpetian A, Tseng B, Ortiz F, Fitten J, Cummings JL, Bartzokis G: Diffusion tensor imaging in preclinical and presymptomatic carriers of familial Alzheimer's disease mutations. *Brain* 2007;130:1767–1776.